Diffusive dynamics of ordered solutions of apoferritin near the structure factor peak

2003 J. Phys.: Condens. Matter 15 S197

(http://iopscience.iop.org/0953-8984/15/1/325)

INSTITUTE OF PHYSICS PUBLISHING JOURNAL OF PHYSICS: CONDENSED MATTER

J. Phys.: Condens. Matter **15** (2003) S197–S204 PII: S0953-8984(03)55432-7

Diffusive dynamics of ordered solutions of apoferritin near the structure factor peak

Wolfgang Häußler and Bela Farago

Institut Laue-Langevin, F-38042 Grenoble, France

E-mail: haeussle@ill.fr

Received 31 October 2002
Published 16 December 2002
Online at stacks.iop.org/JPhysCM/15/S197

Abstract

Aqueous solutions of apoferritin, which consists of 24 proteins assembled into a spherical shell (outer diameter 12 nm), represent highly monodisperse systems. In low-salt solutions, a pronounced peak in the static structure factor $S(q)$ indicates intermolecular interactions due to the net negative charge (pH ≈ 5) of apoferritin. We have investigated both the structure and dynamics of ordered solutions for the first time in the vicinity of the $S(q)$ peak at q^*. Coherent small-angle neutron scattering experiments were performed at the Institute Laue-Langevin (Grenoble) and the dynamics was studied using the high-resolution neutron spin echo spectrometer IN15. The dynamics at $q > q^*$ coincides with extrapolated results of previous experiments. For low-salt solutions, the normalized intermediate-scattering function has a shape that qualitatively resembles that of $S(q)$ in the vicinity of q^*. However, the inverse effective diffusion constant differs quantitatively from $S(q)$ below q^*.

(Some figures in this article are in colour only in the electronic version)

1. Introduction

During the last few decades, various studies on complex fluids have been performed, especially on colloidal suspensions [1–3]. In order to describe the structure and dynamics of charged systems, rescaling procedures were developed [4]. For systems of very small polyelectrolytes, special descriptions have been applied [5, 6]. Increased complexity of structural properties results from interactions deviating from pure repulsion [7–9]. Still controversial is the question of whether there is attraction even between like-charged polyions [10–12]. The structural and dynamic picture of polyelectrolytes can be substantially influenced by polydispersity effects being hard to avoid in synthetic samples [13, 14]. High monodispersity (i.e., identical molecular weight, size, shape and charge of the polyions) is available in biological systems, for example proteins in solution [15].

0953-8984/03/010197+08$30.00

The size of synthetic colloidal particles can be controlled by the synthesis. Thus, scales of length and time can be adapted to various experimental techniques. In contrast, scattering studies resolving structures built up of nm-sized biological particles are restricted to ones using x-ray and particle (neutron) beams. Moreover, translational diffusive dynamics scales with the square of the scattering vector q, and is found typically in the ns range when q corresponds to nm resolution. While the resolution of 'low-q' light scattering techniques matches to colloidal diameters of 50–300 nm, the only technique resolving both nm length scales and ns timescales is the neutron spin echo (NSE) method [16].

In this paper, we present the results of NSE and small-angle neutron scattering (SANS) studies on apoferritin in solution ($M_W = 450$–475 kDa, outer diameter 12 nm) [17, 18]. The apoferritin shell carries net negative charge at pH ≈ 5 [19] which ensures solubility in water. Moreover, due to electrostatic interactions, ordering over several intermolecular distances was found, reflected in a pronounced peak in the static structure factor $S(q)$ at the q-value q^* [18]. Near the freezing transition, temperature-dependent crystalline clustering was reported [17]. Investigations of the dynamics in apoferritin solutions are scarce. While earlier studies were performed at intermediate ionic strength [19], we recently performed photon correlation spectroscopy (PCS) on low-salt solutions and found complex dynamical behaviour [18]. The diffusive dynamics is influenced by electrostatic interactions, and in the long-time diffusion, slow dynamics appears. In the present work, the dynamics of apoferritin solutions is investigated in the q-range near q^*, in contrast to earlier studies, which restricted investigation to low q-values [18, 19]. By means of the NSE technique, being complementary to PCS, the structures built up of the relatively small apoferritin molecules in solution are accessible; thus, the impact of the structure on the dynamics can be studied. Special data analysis takes into account the wavelength spread used as usual in the NSE technique. We find that the shape of $S(q)$ is reflected in the dynamics; however, the diffusion at $q < q^*$ is hindered, indicating the existence of hydrodynamic interactions. In the present work, we question the similarity of apoferritin to a colloidal particle. The peculiarities of this nm-sized system, being its small size, small polydispersity and the intermolecular interaction potential, characterized by the soft protein shell carrying charges of both signs leading to the findings reported in [17–19], have, however, no particular impact on the dynamical picture found by the NSE technique. These experiments are novel; to our knowledge there has been no previous (NSE) study on colloidal-like biopolymers. The present work is mainly restricted to a pure experimental study. Comparison of the data with theoretical concepts is a task for the future. The paper is organized as follows. Section 2 gives a short explanation of the formula needed. Section 3 describes the experimental techniques and the method of sample preparation. Section 4 reports and discusses the NSE results and in section 5 final conclusions are drawn.

2. Theory

Static and dynamic properties of many-particle systems can be described on the basis of the coherent intermediate-scattering function [20]

$$I(q,t) \propto \left\langle \sum_{i=1}^{N} \sum_{j=1}^{N} \exp(\mathrm{i}\boldsymbol{q} \cdot (\boldsymbol{r}_i(0) - \boldsymbol{r}_j(t)) \right\rangle, \tag{1}$$

where N is the number of particles in the scattering volume and $\boldsymbol{r}_i(t)$ is the position of particle i at time t. The brackets denote the equilibrium ensemble average.

$I(q) \equiv I(q,0)$ describes the static structure of the system. For a monodisperse ensemble of spherically symmetric particles, $I(q)$ factorizes as [21]

$$I(q) \propto F^2(q)S(q) \tag{2}$$

with the particle form factor $F^2(q)$ and the static structure factor $S(q)$. For a spherical shell, the form factor amplitude F is given by [21]

$$F(q; r_1, r_2) = 3\frac{(\sin(qr_1) - qr_1\cos(qr_1)) - (\sin(qr_2) - qr_2\cos(qr_2))}{q^3(r_1^3 - r_2^3)} \tag{3}$$

with the outer radius of the sphere r_1, the inner radius of the sphere r_2 and the absolute value of the scattering vector q.

For classical diffusion of non-interacting spherical particles in a solvent, the normalized intermediate-scattering function (1) is given by

$$S(q, t) = \exp(-q^2 D_0 t) \tag{4}$$

with the Stokes–Einstein free-particle diffusion constant

$$D_0 = \frac{kT}{6\pi\eta a} \tag{5}$$

where k is the Boltzmann factor, η is the viscosity of the solvent and a is the radius of the spheres.

In the case of interacting particles, $S(q, t)$ can be expanded at short times as

$$\ln(S(q, t)) \approx -D_{\text{eff}} q^2 t + \frac{\mu_2}{2}t^2 + \frac{\mu_3}{6}t^3 \tag{6}$$

with the effective diffusion coefficient $D_{\text{eff}}(q)$ and the higher cumulants $\mu_{2,3}$.

This theoretical description is based on the assumption that the timescale of the experiment exceeds the short-time fluctuations of the dissolved particles due to collisions with solvent molecules. This assumption is justified when the experiment is sensitive to times above the Brownian relaxation time $\tau_B \approx m/6\pi\eta a$, where m is the mass and a the radius of the particle. For a particle of $a = 6$ nm dissolved in aqueous solvent at room temperature, the Brownian relaxation time amounts to a few nanoseconds. A similar rough estimation of the interaction time τ_I needed for a non-interacting sphere of radius $a = 6$ nm to diffuse a distance roughly equal to its radius in water gives $\tau_I \approx a^2/D_0 > 1\ \mu$s. This time exceeds the maximum spin echo times available (see the next section) while, on the other hand, even the smallest spin echo times used were larger than τ_B.

3. Experimental details

3.1. Samples

Apoferritin from horse spleen was purchased from SIGMA (concentration 51 mg ml^{-1}, sodium salt content 100 mM). Small amounts of the stock solution (3 ml) were centrifuged with 8000 rpm using 10 kD filters (Millipore 'Ultrafree'). First, the solution was concentrated by a factor of 5–6. Then, dialysis to D_2O was accomplished by addition of 3 ml D_2O and subsequent centrifugation. In order to produce 99.9% deuterated solvent, this was repeated 4–5 times. Finally, different amounts of pure or salty D_2O (NaCl, Riedel de Haen) were added. The concentration was determined by weighing defined volumes of the protein solution before and after dialysis. The ranges of both the protein and salt concentrations are the same as those for the systems studied in H_2O [18]. We conclude that the pH values are in the range 5.1–5.3.

For the neutron scattering measurements, 1–2 ml of the sample solution were poured into quartz cuvettes (Hellma, Germany, 30 × 30 mm^2). The sample thickness was 1–2 mm for all sample solutions. The transmission through empty cuvettes was 95%; the transmission of the samples was 69–82%. The polarization of the scattered intensity normalized by the polarization measured with graphite was 0.97–1. Therefore, incoherent scattering can be neglected, and collective dynamics is measured by the NSE experiments.

3.2. Neutron spin echo measurements

The NSE measurements were performed at the Institute Laue-Langevin (ILL, Grenoble) at IN15. We used wavelengths of 14.7–15.2 Å with a wavelength spread of 15% (FWHM). The maximum field integral was 2.7×10^5 Oe cm and the maximum spin echo time $\tau_{SE} = 190$ ns. The maximum divergence of the beam was 0.17 mrad. The scattering vector covered the range $0.02\ \text{Å}^{-1} < q < 0.1\ \text{Å}^{-1}$. A multidetector with 32×32 pixels was used, distributed into 3–6 sections. The sample temperature was 293 K.

The data were corrected for background scattering from the sample cell and solvent. The normalized intermediate-scattering function was extracted from the spin echo measurements divided by the elastic polarization. The q-smearing was corrected for the beam cross-section, wavelength spread and area of the detector sections.

3.3. Neutron small-angle measurements

SANS data were extracted from the quasielastic data measured at IN15 in order to get static and dynamic data with identical q-smearings. The data were corrected for background scattering analogously to the dynamic data. By choosing overlapping detector positions, effects of varying detector efficiency were corrected.

4. Results and discussion

The measured SANS intensities are depicted in figure 1. The apoferritin concentrations of the high-salt sample solutions were 26 mg ml^{-1} (volume fraction $\phi = 2.5\%$) and 156 mg ml^{-1} ($\phi = 15\%$). The salt contents were 21 and 130 mM NaCl. Within the statistical errors, the low-concentration data are indistinguishable from the data for the 156 mg ml^{-1} apoferritin solution, indicating negligible interparticle interactions at high salt content. The SANS data of figure 1 are compared with a fit to SAXS data from [18] ($\phi = 10\%$, salt content 220 mM). In general, SAXS and SANS data fit well outside the first minimum demonstrating that the proteins are of similar shape. In figure 1, a model function is also shown, according to equation (3), after having been modified in order to allow for small, Gaussian-distributed deviations $\Delta r_{1,2}$ of the outer and inner radius from their mean values and taking into account the neutron wavelength spread (15%). The best fit resulted with $r_1 = (6.06 \pm 0.2)$ nm, $r_2 = (3.83 \pm 0.2)$ nm, $\Delta r_1/r_1 = 4.3\%$ and $\Delta r_2/r_2 = 5\%$, in fair agreement with the SAXS values ($\Delta r_1/r_1 = 3.8\%$, $\Delta r_2/r_2 = 2.9\%$ [18]). Thus, it is reasonable to assume that the system studied resembles the system from [18]. Moreover, the reported polydispersity is mainly due to elastic deformations of the protein shell, so the mean size is even more regular [18].

The results of the SANS experiments on low-salt solutions (0.01 mM NaCl) are also shown in figure 1. The scattered intensity is characterized by a pronounced peak. The peak shifts to higher q-values and the height of the maximum increases with increasing apoferritin concentration. The position of the peak for the high-concentration data ($q^* = 0.037\ \text{Å}^{-1}$) agrees with the mean distance calculated from the number concentration, while the lower-concentration data show a slight difference (0.035 Å^{-1}; calculated: 0.033 Å^{-1}).

Figure 2 displays the NSE relaxation rates extracted by means of a single-exponential fit to the NSE data from high-salt apoferritin solutions compared to PCS results [18]. After scaling the PCS data with a factor due to the different viscosities of H_2O and D_2O, the SANS and PCS data agree very well. Over three decades of q-range, they give the diffusion constant of apoferritin in D_2O: $D_0 = 2.5 \times 10^{-7}$ cm s^{-1}. The hydrodynamic radius a of apoferritin (equation (5)) rises to 6.9 nm, which is slightly larger than r_1. This deviation, consistent with literature values, is due to the hydration shell around the molecule in aqueous solution [22–25].

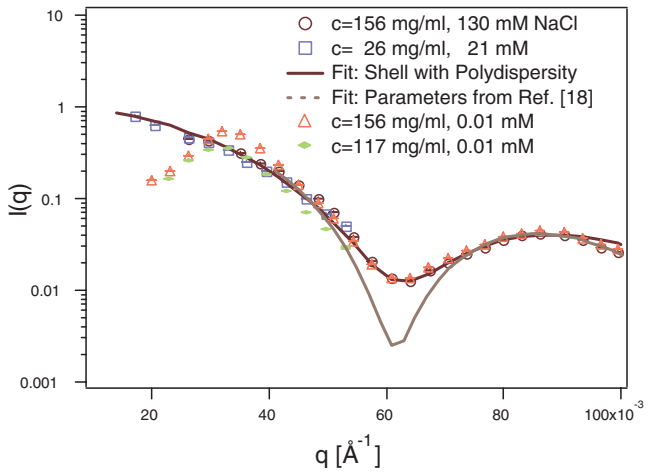

Figure 1. SANS intensities from high-salt and low-salt apoferritin solutions are shown together with a model function (curve) for spherical particles obtained using the parameters from the best fit to the high-salt data (see the text). The dashed curve is the shell fit function with parameters taken from [18].

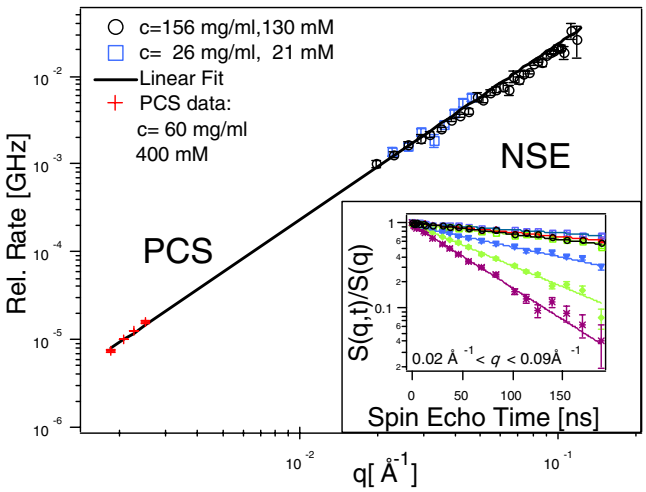

Figure 2. Relaxation rates measured by the NSE technique in non-interacting particle solutions compared with relaxation rates measured by PCS [9] after having been scaled with the factor $f = 1.251$ due to the different viscosities of H_2O and D_2O. Inset: the logarithm of the intermediate-scattering functions $S(q, t)$ measured on the sample of 156 mg ml^{-1} apoferritin concentration and 0.01 mM salt content. $\ln(S(q, t))$ is linear over the whole range of spin echo times measured and for all curves taken at different q-values.

The inset of figure 2 shows the NSE data for the sample of 156 mg ml^{-1} apoferritin concentration and 0.01 mM salt content. Also, these low-salt NSE data were fitted by means of a single-exponential function. As this Gaussian approximation is valid only in the limit $t > 0$ (equation (6)), we also fitted the data with a function taking into account the higher cumulants. However, the fitted values for the first cumulant did not differ from the values extracted from the single-exponential fit, and the higher orders were close to zero. Moreover, it can be seen clearly from figure 2 that the logarithm of the intermediate-scattering function is

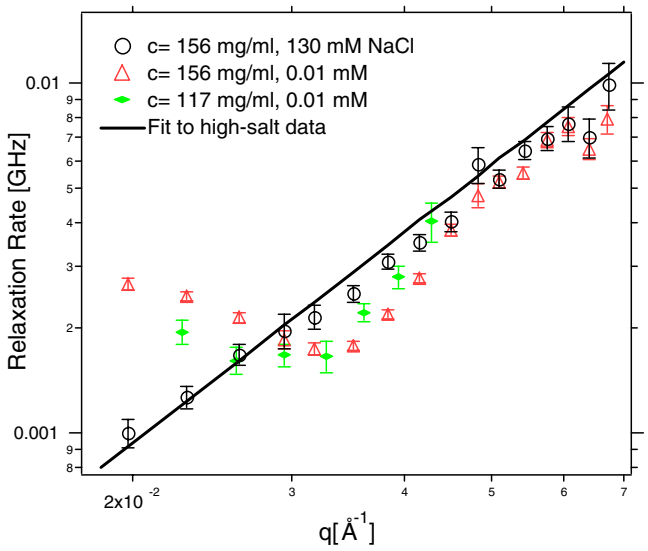

Figure 3. Relaxation rates for the low-salt samples from figure 1. At low q, the dynamics is much faster and the relaxation rate Γ does not follow the free diffusion dependence $\Gamma \sim q^2$. In addition, the Γ curves cross the free-particle diffusion curve (line). Following the shape to higher q-values, the relaxation turns towards the free-particle diffusion line.

linear over the whole range of spin echo times measured and for all $S(q, t)$ curves at different q-values.

The dynamic data from the NSE technique for the low-salt samples from figure 1 are shown in figure 3. At low q, the dynamics is much faster and the relaxation rate Γ does not pursue the free diffusion dependence $\Gamma \sim q^2$. In addition, the relaxation rate crosses the free-particle diffusion line which is added to the plot. Following the shape to higher q-values, the relaxation turns towards the free-particle diffusion line. This behaviour is expected: the spatial resolution of the high-q data is sensitive to small-scale dynamics. Therefore, the intermediate-scattering function (equation (1)) reflects self-correlations [15].

The SANS intensity $I(q)$ shown in figure 1 depends on both the structure factor $S(q)$ resulting from the interparticle ordering and the form factor of apoferritin $F^2(q)$. For spherically symmetric particles these two contributions can be separated easily, because the scattered intensity is given by the product of the form factor and the structure factor (equation (2)). Due to the wavelength spread, this formula is not exactly valid in our case, because the q-smearing resembles a summation which is present both in the low-salt $I(q)$ data and in the form factor data. However, the error is very small, because the dominant structures in the curves are much broader than the relative bandwidth. The structure factor $S(q)$ calculated according to equation (2) is shown in figure 4. Comparison between $I(q)$ and $S(q)$ shows that the $S(q)$ maxima are shifted slightly to higher q-values, which is due to the negative slope of the form factor in the q-range under consideration.

Figure 4 also shows the normalized inverse effective diffusion coefficient D_0/D_{eff}. As expected [15], a maximum appears corresponding to the $S(q)$ peaks. Especially for the concentration of 117 mg ml^{-1}, the coincidence of the static and dynamic data is evident. But for the higher-concentration data also, the positions, heights and shapes of the peaks are similar. However, at low q-values, the dynamic data are significantly above the static data. This indicates hydrodynamic interactions slowing down the dynamics.

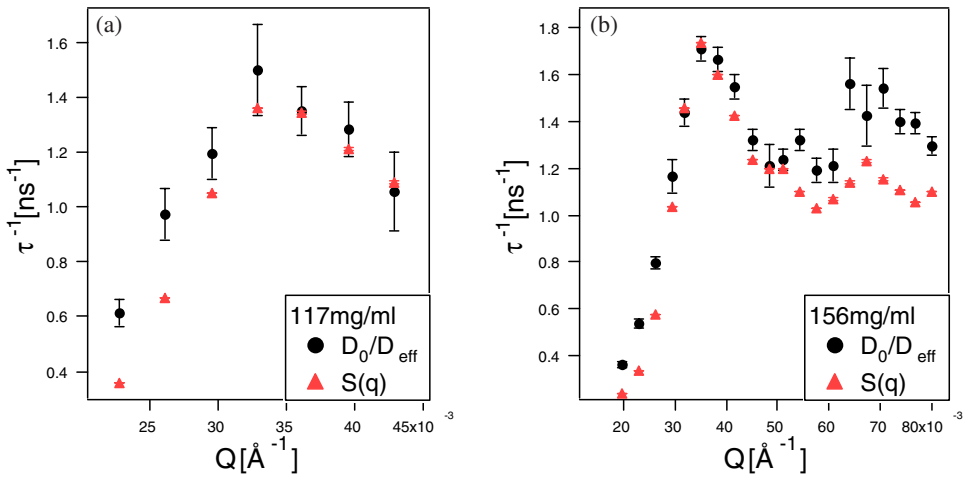

Figure 4. The normalized inverse effective diffusion coefficient $D_0/D_{\rm eff}(q)$ is displayed together with the structure factor $S(q)$ calculated by division of the intensity data by the form factor (figure 1). Low-salt data are shown for two protein concentrations: (a) 117 mg ml^{-1}, (b) 156 mg ml^{-1}. There are no qualitative differences between the static and dynamic data. The positions, heights and shapes of the peaks are similar.

5. Conclusions

We performed neutron scattering experiments on apoferritin in solutions of varying protein and salt content. The shape of single apoferritin molecules is reflected in a shell-like form factor measured by means of SANS for high-salt solutions. Under the same solvent conditions, the proteins show classical diffusion. The free-particle diffusion constant was found to agree with the literature and previous PCS data. We conclude from the high-salt data that the sample consisted of apoferritin monomers of well-defined size and shape. Furthermore, the apoferritin solutions investigated under low-salt conditions are ordered, as reflected in the appearance of a structure factor peak which shifts to higher q-values with increasing protein concentration. In summary, apoferritin in solution is acting as a colloid whose interparticle interactions can be controlled by means of the solvent salt content.

The dynamical picture of the ordered solutions as measured by the NSE technique reflects the influence of both electrostatic and hydrodynamic interactions on the dynamics. At q^*, strong spatial correlations reflected in the structure factor peak slow down the decay of the normalized intermediate-scattering function. At q-values smaller than q^*, hydrodynamic interactions hinder the dynamics. These results agree with the behaviour of the charged colloidal systems reported in [14, 26, 27]. Thus, not only the structure, but also the dynamical picture of low-salt apoferritin solutions measured by the NSE technique confirms the similarity of these protein system to colloidal suspensions.

Finally, the NSE data presented here can supplement previously reported PCS results [18], as in the light scattering 'low-q' range, slow dynamics was found. Since it was predicted that strong hydrodynamic interactions can cause deviations in the long-time decay of large-scale fluctuations from the short-time dynamics at small q-values [15], the results for the hydrodynamic function reported here could support the assumption that the slow mode reported for interacting apoferritin systems is of hydrodynamic nature.

However, the complex dynamical picture of apoferritin in solution, like the behaviour at the relatively low PCS q-values [18, 19], prevents simple identification of these systems

with model colloidal systems, though colloidal-like behaviour, both in high-salt solutions and low-salt solutions, near the structure factor peak is reported in the present work. Instead, a picture doing justice to both the low-q and high-q phenomena is necessary.

References

[1] Naegele G 1996 *Phys. Rep.* **272** 215
[2] Brown J, Pusey P N, Goodwin J W and Ottewill R H 1975 *J. Physique* A **8** 664
[3] Hansen J-P and Hayter J B 1982 *Mol. Phys.* **46** 651
[4] Banchio A J, Naegele G and Bergenholtz J 2000 *J. Chem. Phys.* **113** 3381
[5] Lin S C, Lee W I and Schurr M J 1978 *Biopolymers* **17** 1041
[6] Förster S, Schmidt M and Antonietti M 1990 *Polymer* **31** 781
[7] Tata B V R and Ise N 1996 *Phys. Rev.* B **54** 6050
[8] Stevens M J, Falk M L and Robbins M O 1996 *J. Chem. Phys.* **104** 5209
[9] Sear R P 1999 *J. Chem. Phys.* **111** 4800
[10] Schmitz K S 1997 *Langmuir* **13** 5849
[11] Allahyarov E, D'Amico I and Loewen H 1998 *Phys. Rev. Lett.* **81** 1334
[12] Klein R, Von Grünberg H H, Bechinger C, Brunner M and Lobaskin V 2002 *J. Phys.: Condens. Matter* **14** 7631
[13] Sheu E Y, Chen S-H, Huang J S and Sung J C 1989 *Phys. Rev.* A **39** 5867
[14] Phalakornkul J K, Gast A P, Pecora R, Naegele G, Ferrante A, Mandl-Steininger B and Klein R 1996 *Phys. Rev.* E **54** 661
[15] Pecora R 1985 *Dynamic Light Scattering* (New York: Plenum)
[16] Mezei F 1980 *Neutron Spin Echo* (Berlin: Springer)
[17] Kilcoyne S H, Mitchell G R and Cywinski R 1992 *Physica* B **180/181** 767
[18] Häußler W, Wilk A, Gapinski J and Patkowski A 2002 *J. Chem. Phys.* **117** 413
[19] Petsev N and Vekilov P G 2000 *Phys. Rev. Lett.* **84** 1339
[20] Lovesey S W 1986 *Theory of Neutron Scattering from Condensed Matter (Nuclear Scattering vol 1)* (Oxford: Oxford University Press)
[21] Pedersen J S 1997 *Adv. Colloid Interface Sci.* **70** 171
[22] Harrison P M and Arosio P 1996 *Biochim. Biophys. Acta* **1275** 161
[23] Brown W (ed) 1993 *Dynamic Light Scattering: the Method and some Applications* (Oxford: Clarendon)
[24] Israelachvili J and Wennerstroem H 1996 *Nature* **379** 219
[25] Sivergun D I, Richard S, Koch M H J, Sayers Z, Kuprin S and Zaccai G 1998 *Proc. Natl Acad. Sci. USA* **95** 2267
[26] Philipse A P and Vrij A 1988 *J. Chem. Phys.* **88** 6459
[27] Haertl W, Beck Ch and Hempelmann R 1999 *J. Chem. Phys.* **111** 8209